Stabilizing DFB laser injection-locked to an external polarization maintaining optical fiber ring cavity

Ivan Panyaev[a], Pavel Itrin[a], Dmitry Korobko[a], Ivan Chapalo[b], Patrice Mégret[b], Andrei Fotiadi[b,c]
[a]Ulyanovsk State University, 42 Leo Tolstoy Street, Ulyanovsk, 432970, Russia.
[b]Optoelectronics and Measurement Techniques Unit, University of Oulu, 90570 Oulu, Finland.
[c]University of Mons, Boulevard Dolez 31, 7000 Mons, Belgium.

ABSTRACT

We report on linewidth narrowing and stabilization of semiconductor DFB laser implemented through its self-injection locking to an external fiber ring cavity in conjunction with an active optoelectronic feedback circuit controlled by a simple low-cost USB-DAQ card. The system enables narrowing of the DFB laser linewidth below ~0.5 kHz and drastically reduced the laser phase noise. Specifically, the laser configuration is fully spliced from the polarization maintaining (PM) single-mode optical fiber that exhibits significantly improved stability against the environment noise. Drastic narrowing of the DFB laser linewidth down to ~310 Hz and a phase noise less than –100 dBc/Hz (>30 kHz) are achieved with the PM fiber ring cavity built from a single fiber coupler. The reported PM laser configuration is of great interest for many laser applications where a narrow sub-kHz linewidth, simple design and low cost are important.

Keywords: Narrow-band fiber lasers; self-injection locking; fiber ring cavity.

1. INTRODUCTION

Compact cost-effective laser sources with tunable coherency are of the great demand for a number of potential applications [1-9]. Among them are high-resolution spectroscopy, phase-coherent optical communications, microwave photonics, coherent optical spectrum analyze, and distributed fiber optics sensing [10-24]. Therefore, linewidth narrowing and stabilization of semiconductor laser light generation are of topical research interest. Linewidths of free-running DFB semiconductor lasers typically range from a few MHz. The self-injection locking to an external fiber cavity is an efficient method enabling drastic linewidth narrowing and self-stabilization of semiconductor lasers. To provide the effect, a part of the optical radiation emitted by the laser is returned back into the laser cavity thus decreasing the laser threshold at the locked frequency [25]. This relatively simple technique allows to design cost-effective narrow-band laser sources based on standard laser diodes making them an attractive solution in comparison with conventional laser systems based on active feedback. Commonly, self-injection locking laser configurations comprise a narrow bandpass optical filter inside a weak feedback loop [26]. Current progress in this topic is associated with the use of micro-cavity techniques [27, 28]. Employing optical whispering-gallery-mode resonators the linewidth of the semiconductor laser could be decreased down to sub-kHz range in a compact and robust configuration. However, the external cavities used in such systems possessing huge Q-factors (~10^{11}) are not flexible for adjustment and require rather complicate coupling of fiber and non-fiber elements.

Alternatively, all-fiber cavity solution based on long but relatively low-Q-factor fiber-based resonators is able to provide comparable semiconductor laser line narrowing with a low-cost fiber configuration built from standard telecom components [29-33]. In particular, such solutions are of great interest for RF-generation and Brillouin distributed sensing, the same fiber cavity can serve as a nonlinear medium to generate Brillouin frequency-shifted light [34-53]. We have demonstrated significant line narrowing (more than 1000 times) of a conventional low-cost DFB laser locked to an external fiber optic ring resonator [33]. Once locking, any slow change of interferometer mode frequency (due to temperature fluctuations, for example) leads to a simultaneous change of the laser generation frequency.

The main drawback of this technique is its high sensitivity to fluctuations of the configuration parameters and surroundings. Commonly, self-stabilization of the laser operation through injection locking is supported only within a limited range of the laser frequency deviations, typically tens of MHz [30]. Beyond this range even a minuscule fluctuation in the ambient parameters can destabilize lasing causing mode-hopping. As a result, stable laser operation intervals are interrupted by short-time jumps in the lasing intensity caused by laser mode-hopping [33]. Although the precise stabilization of laser pump current and temperature of fiber configuration allows increasing these intervals up to tens of minutes, no simple means permanently stabilizing laser operation in a single longitudinal mode have been reported for a while. Rare mode-hopping events still interrupt frequency locking making many practical laser applications questionable.

In this paper, we make few steps forward in comparison with the previously reported narrow-band laser configurations. New laser design combines a number of advanced laser linewidth narrowing and stabilization mechanisms in a single DFB laser configuration. First, the reported laser configuration is completely spliced from the standard telecom PM fiber components. It makes the laser operation much more resistible to an external laser perturbations and environment noise. Second, we have used the self-injection locking mechanism in conjugation with an additional active optoelectronic feedback circuit extending the range of the laser self-stabilization over ~1GHz [54]. Importantly, the optoelectronic feedback loop just helps to maintain the regime of passive self-injection-locking that makes the major contribution to the laser linewidth narrowing. In terms of the feedback bandwidth, complexity, allocated PC memory the proposed combined solution is much less consuming than the optoelectronic feedback circuits commonly used with single-frequency fiber lasers [55, 56]. And finally, the new laser design comprises an optical fiber ring cavity with the Q-factor that is higher than that used with the self-injection locked fiber lasers earlier. The self-injection locking mechanism provides more than a 1000-fold narrowing of the DFB laser linewidth. Active optoelectronic feedback based on a simple microcontroller ensures long-term stabilization of the laser operation. We have explored key features of the laser operation with and without the active feedback, in particular, demonstrating a control and tuning of the laser generation linewidth. The laser stabilization dynamics, linewidth narrowing, and phase noise reduction in the new fiber laser configuration are experimentally explored.

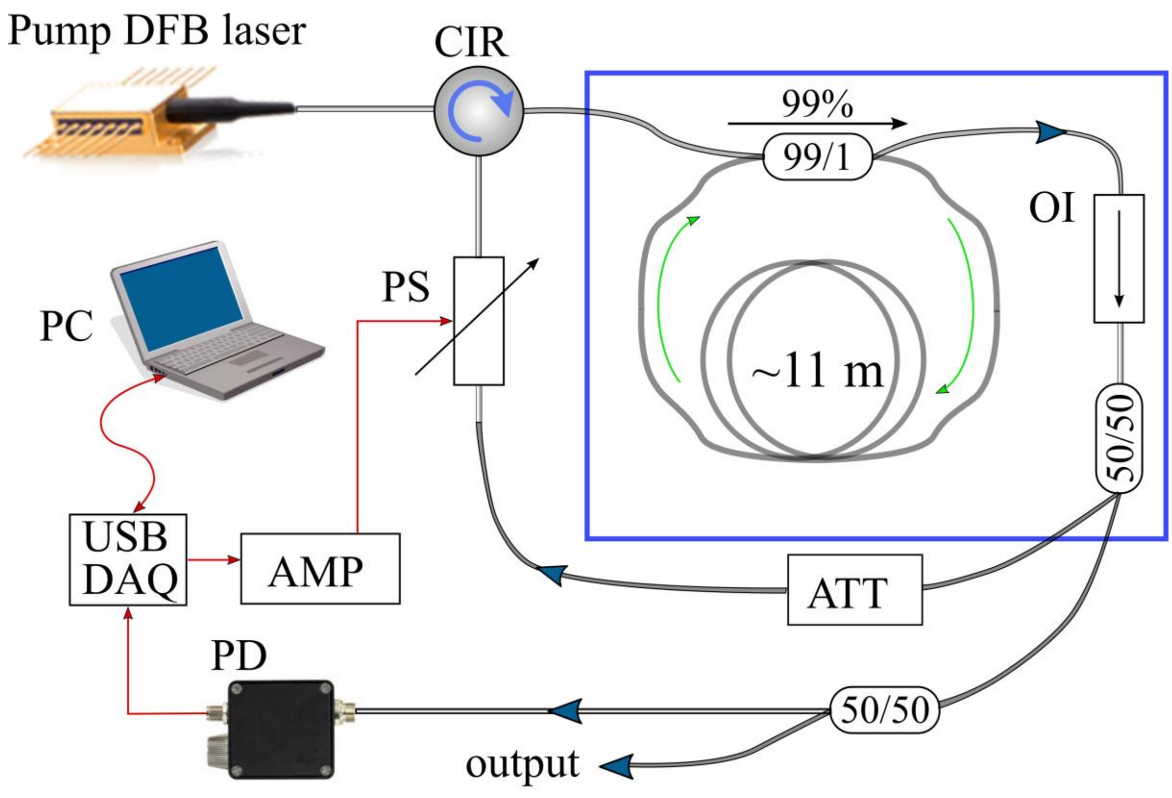

Figure 1. Schematic illustration of the experimental configuration; CIR – circulator, OI – optical isolator, ATT – attenuator, PS – phase shifter, USB-DAQ - microcontroller, PD –photodetector, AMP – control signal amplifier. The blue solid line indicates the contour of the thermal and vibration insulation box.

2. LASER CONFIGURATION

The experimental laser setup is shown in Fig. 1. It is totally spliced from standard PM fiber telecom components. A standard distributed feedback (DFB) laser diode (Mitsubishi FU-68PDF-5) supplied by a -30 dB built-in optical isolator emits radiation with a maximal power of ~15 mW at ~1552 nm in linear polarization. The light emitted by the laser passes an optical circulator and is introduced into a high-Q ring resonator. The high-Q ring resonator is spliced from a single coupler (99/1) and comprises ~11m length of standard PM fiber (Nufern PM1550-XP). In order to implement the injection locking mechanism the laser radiation passed the ring resonator returns back into the DFB laser cavity thus providing passive feedback to the laser operation. The fiber feedback loop comprises the optical isolator (OI), 50/50 coupler, attenuator (ATT) and phase-shifter (PS). The 50/50 coupler redirects a part (50%) of the laser power passing through the feedback loop to the photodetector and laser output. The built-in optical isolator eliminates the effects of uncontrollable back reflections and simultaneously reduces the value of a feedback power obtained from the external fiber optic ring resonator. The portion of the feedback power returned to the DFB laser cavity is controlled by ATT. The optical isolator (OI) isolates the DFB laser from undesirable back reflections from the fiber faces. The laser operation is monitored by a fast photodetector (PD, Thorlabs DET08CFC, 5 GHz, 800 - 1700 nm). A fiber phase-shifter based on the thermo-optical effect (Phoenix Photonics VPS150-15-PM-2-1) is attached to the feedback loop and driven by a low-cost USB Multifunction DAQ (based on the Arduino board) connected with a PC. The active feedback circuit helps the laser to maintain the desired laser operation in self-injection locking regime. The fiber configuration is placed into a foam box stabilized at ~25 ◦C to protect the laser system from the laboratory environment. A fast photodetector detects the optical signal at the laser output. The signal from the photodetector is used as an error signal of the active feedback circuit. The active feedback circuit tends to keep the feedback signal at the desired level applying an appropriate voltage to the fiber phase-shifter. Additional thermal control (also based on the Arduino board) is applied to the laser box as a whole to control the voltage applied to the phase-shifter, in particular, to keep it within the dynamic range. A delayed self-heterodyne technique has been employed to measure the linewidth of radiation emitted by the laser at different stabilization regimes. An all-fiber disbalanced Mach–Zehnder interferometer with a 50 km delay fiber and 80 MHz phase modulator supplied by polarization controller is used for this purpose[57]. The beat signal from the interferometer is detected by a ~5 GHz photodiode and RF spectrum analyzer.

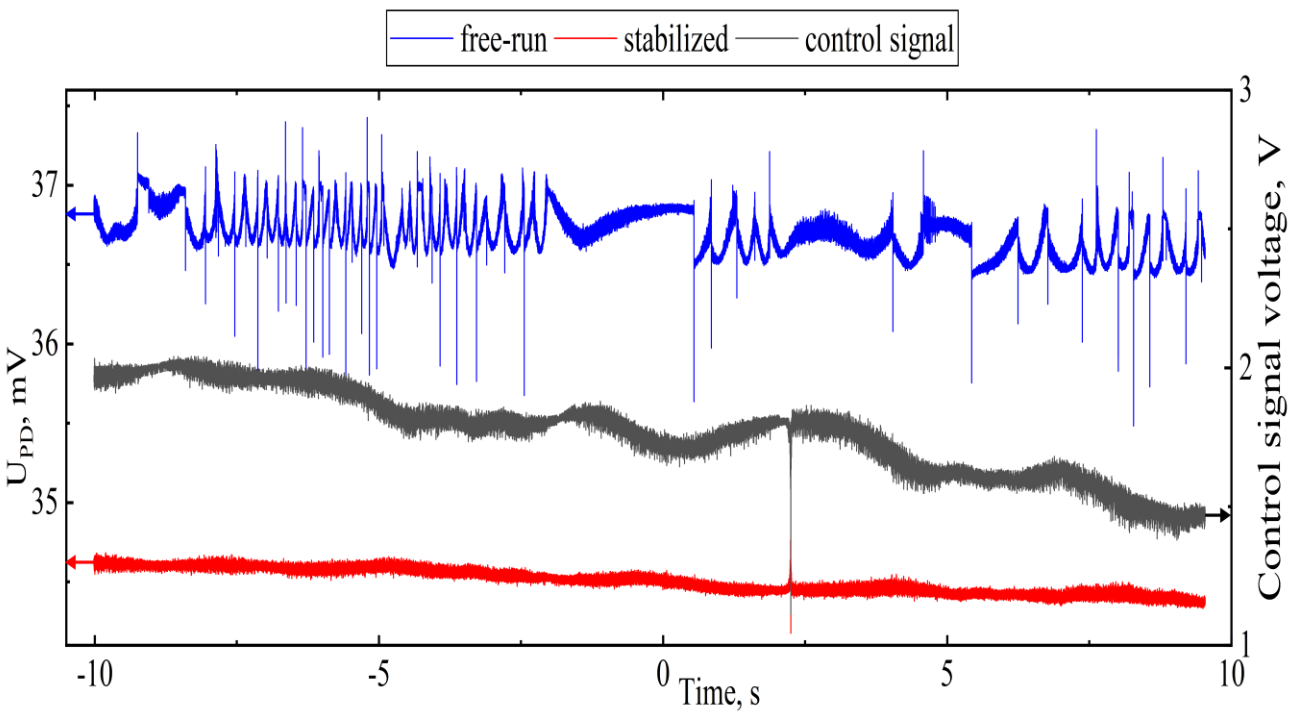

Figure 2. Typical oscilloscopic traces of the free-running DFB laser (blue curve), stabilized self-injection locked laser (red curve) and control signal (black curve).

2. EXPERIMENTAL RESULTS: LASER POWER BEHAVIOUR

When the passive feedback loop is open, the laser operates in a free-running regime. Figure 2 (blue curve) shows a typical oscilloscope trace recorded with the free-running laser power passed through the high-Q fiber ring cavity. One can see the recorded trace exhibits a lot of peaks caused by extended DFB laser frequency variations. The closed feedback loop forces the laser to operate in the self-injection locking regime resulting in suppression of the intensity fluctuations. In this case the laser operating frequency is locked to the resonance frequency of the high-Q cavity resonance. Slow changes of the ring cavity frequency caused by the environment noise (acoustic and temperature) result in synchronous changes of the DFB laser frequency. Any deviations of the DFB laser frequency from the ring cavity resonant frequency increases the laser output power recorded by the photodetector. The aim addressed to the active feedback circuit is to keep the signal recorded by the photodetector as low as possible affecting the phase delay in the optical feedback loop.

Figure 2 show oscilloscope traces recorded with the stabilized laser output power (red curve) and with control signal applied to the phase-shifter (black curve). For the laser operating without electronic feedback the laser frequency is not locked to the ring resonance. The electronic feedback circuit is trying to maintain the laser power detected at the detector (it is used as an error signal for the active circuit) fixed to its minimal value. One can see that the DFB laser frequency is always locked to the ring cavity resonance providing a stable laser operation recorded by the photodetector (red curve). The self-injection locking mechanism in combination with optoelectronic feedback (see, black curve) perfectly works against the environment noise. Sometimes, the stabilized laser behavior could be interrupted by a short mode-hopping event provoked by the environment noise. A typical time of the system recovery provided by active electronic feedback is $\tau_L \sim 0.2\, s$.

Another source of the laser instabilities is an extended drift of environment temperature. The environmental temperature variations affect both the ring cavity and feedback loop fiber lengths moving the mutual position of the resonant ring cavity and feedback loop frequencies. The electronic feedback circuit works against the temperature noise trying to maintain their equality. To this end, it controls the phase delay in the optical feedback loop smoothly changing the voltage applied to the phase-shifter. The dynamical range of the phase-shifter is limited by $\pm 75\, rad$. When this limit is exhausted, the phase must be reset by an integer number of circles. Such jumps of the control signal destabilize the laser for a short time. A typical time of the stabilized laser operation in the laboratory environment (between two jumps of the control signal) is ~30 min. To avoid this instability an additional thermal control is applied to the laser box as a whole. It used to keep the feedback circuit within its dynamic range ensuring long-term laser operation stability.

3. EXPERIMENTAL RESULTS: OPTICAL SPECTRA

The spectral performance of the laser operation is demonstrated in Fig. 3. It compares the self-heterodyne optical spectra [57-62] recorded with the laser configuration with the free-running DFB laser (open optical feedback loop) and with the DFB laser stabilized by optical and electronic circuits. The experimental spectra shown in Fig. 3 are averaged over 10 realizations each. The spectra are centered around ~80 MHz. One can see that the stabilization of self-injection locking causes 1000-fold narrowing of the laser spectrum. The narrower spectrum of the stabilized laser exhibits oscillations in the wings evidencing that the laser coherence length is much longer than the interferometer delay fiber [58]. To proceed the measured data, we use the method based on the decomposition of the self-heterodyne spectra into Gaussian and Lorentzian contributions [59, 61]. In this approach, the laser's line is thought to be Gaussian in the range near the top, and Lorentzian in the wings. Long delay fiber results in considerable broadening of the self-heterodyne spectrum due to the 1/f frequency noise. The convolution with the acquired 1/f noise causes overestimation of the natural laser linewidth, if it is estimated from the 3-dB width of self-heterodyne spectrum as commonly used [57]. Since, the 1/f noise contributes Gaussian broadening mostly pronounced near the top of the laser spectrum, the estimation by the 20-dB width of self-heterodyne spectrum is closer to the natural laser linewidth, however, the result is still overestimating [59]. The measured self-heterodyne spectrum is actually the Voigt profile, i.e., the convolution of the Lorentzian and Gaussian spectra. The Lorentzian and Gaussian contributions can be evaluated by fitting the measured self-heterodyne spectrum by the Voigt profile. Figure 3 shows the fitting Voigt profiles obtained using the algorithm described in Ref. [61]. One can see that the fitting is applied just to the highest points in the wings ensuring upper values of the Lorentzian laser linewidths estimated for two laser outputs. The Lorentzian laser linewidth Δw_L is a half of the Lorentzian width (FWHM) w_L of self-heterodyne spectrum and the Gaussian component Δw_G is $\sqrt{2}/2$ times the Gaussian linewidth

(FWHM) w_G of self-heterodyne spectrum [59]. Therefore, the Gaussian laser linewidths are found to be narrower than 1.3 MHz and 3.8 kHz for the free and stabilized laser, respectively. And the natural Lorentzian laser linewidths are found to be narrower than 430 kHz and 310 Hz for the free and stabilized laser, respectively.

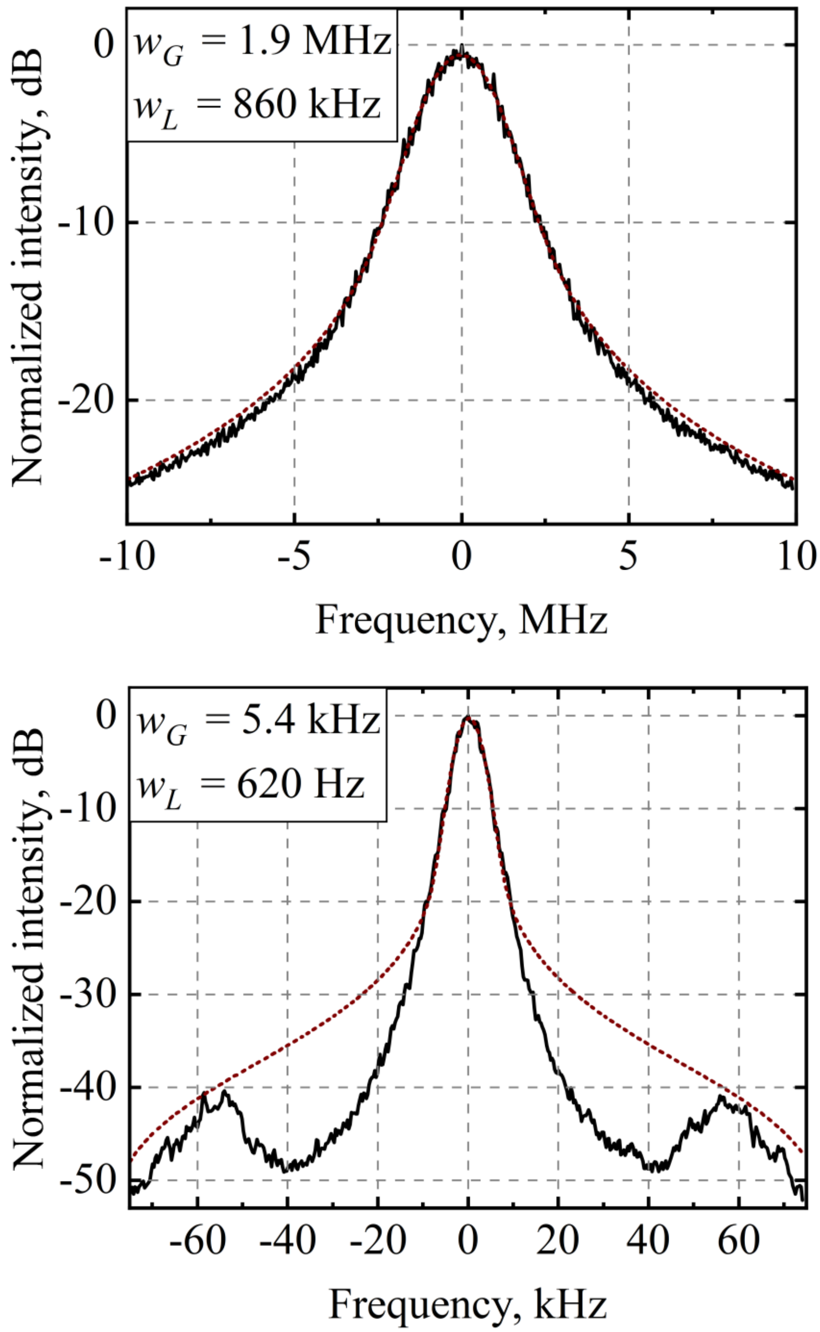

Figure 3. Delayed self-heterodyne spectra of the free-running DFB laser (a) and the laser operating in the self-injection locking mode (b). The measured spectra (black) and their fitting Voigt profiles (red) with the Gaussian and Lorentzian linewidths (FWHM) used as the fitting.

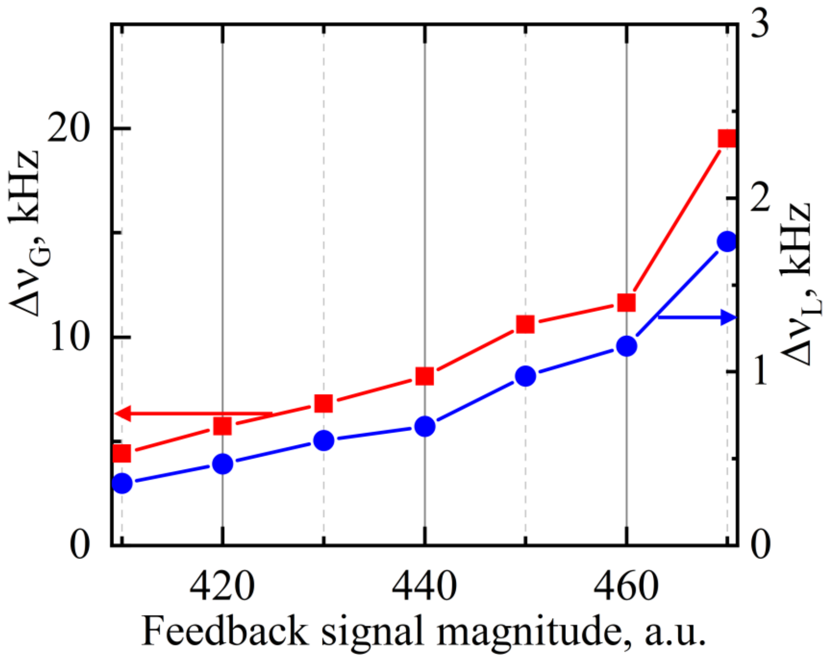

Figure 4. Dependence of the laser linewidth in the self-injection locking mode on the magnitude of the feedback signal shows the ability to control the laser linewidth

4. LASER LINEWIDTH TUNING

With built-up feedback loop self-injection-locking regime is established and followed by a drastic (~1000 times) reduction of the Lorentzian laser linewidth down to sub-kHz scale. The minimal laser Lorentzian linewidth recorded in the experiment is ~ 310 Hz. In self-injection locking regime with passive feedback only the laser linewidth maintains its minimal value during 10–100 minutes (depending on environment noise level). The rest time it slowly walks within the range of 3.1 – 3 kHz until mode-hopping event occurs. The efficiency of laser linewidth narrowing could be monitored by detecting the laser power monitored by the photodetector. With the laser operating in free-lasing regime the laser power gets the maximal value. For the laser operating in self-injection-locking regime the power P_B is lower. When the generated laser frequency coincides with one of the ring cavity resonance peaks both the laser linewidth and laser power are minimal. Any detuning of the laser frequency from the cavity resonant peak frequency increases the laser linewidth and decreases the laser power. Therefore, both detuning of the laser frequency from the cavity resonant frequency and laser linewidth could be monitored by the photodetector. When the optoelectronic feedback circuit maintains the laser power fixed to some set value, it keeps the laser linewidth as well fixed. Figure 4 show the measured laser Gaussian and Lorentzian linewidths as functions of the laser power expressed in arbitrary units. So, the applied active feedback circuit could play in the laser configuration a second role granting control and tunability to the laser linewidth.

5. CONCLUSION

In conclusion, we have implemented an active feedback loop based on a low-cost USB-DAQ to the configuration of DFB laser self-injection-locked to an external all-fiber ring resonator extending the frequency deviation range available for self-stabilization. Specifically, the laser configuration is fully spliced from the polarization maintaining (PM) single-mode optical fiber that exhibits significantly improved stability against the environment noise. The reported results enhance our understanding of the self-injection-locking mechanism in semiconductor lasers and open up new possibilities for manipulating and controlling their properties. Particularly, new ability to control and tune the laser linewidth is attractive for many laser applications, including high-resolution spectroscopy, phase coherent optical communications, microwave photonics, coherent optical spectrum analyzer, distributed fiber optics sensing, in particular, phase-OTDR acoustic sensing [63-71].

ACKNOWLEDGEMENTS

The work was supported by the RSF (#23-79-30017). A.F. is supported by the European Union's Horizon 2020 research and innovation programme (H2020-MSCA–IF–2020, #101028712).

REFERENCES

[1] Zhongmin Yang, C. L., Shanhui Xu, Changsheng Yang, [Single-frequency fiber lasers], Springer (2019).
[2] Popov, S. M., Chamorovski, Y. K., Isaev, V. A., Mégret, P., Zolotovskii, I. O., and Fotiadi, A. A., "Electrically tunable brillouin fiber laser based on a metal-coated single-mode optical fiber," Results in Physics **7**, 852-853 (2017).
[3] Popov, S. M., Butov, O. V., Chamorovskiy, Y. K., Isaev, V. A., Kolosovskiy, A. O., Voloshin, V. V., Vorob'ev, I. L., Vyatkin, M. Y., Mégret, P., Odnoblyudov, M., Korobko, D. A., Zolotovskii, I. O., and Fotiadi, A. A., "Brillouin lasing in single-mode tapered optical fiber with inscribed fiber bragg grating array," Results in Physics **9**, 625-627 (2018).
[4] Popov, S. M., Butov, O. V., Chamorovski, Y. K., Isaev, V. A., Mégret, P., Korobko, D. A., Zolotovskii, I. O., and Fotiadi, A. A., "Narrow linewidth short cavity brillouin random laser based on bragg grating array fiber and dynamical population inversion gratings," Results in Physics **9**, 806-808 (2018).
[5] Popov, S. M., Butov, O. V., Bazakutsa, A. P., Vyatkin, M. Y., Chamorovskii, Y. K., and Fotiadi, A. A., "Random lasing in a short er-doped artificial rayleigh fiber," Results in Physics **16**, 102868 (2020).
[6] Popov, S. M., Butov, O. V., Kolosovskii, A. O., Voloshin, V. V., Vorob'ev, I. L., Isaev, V. A., Vyatkin, M. Y., Fotiadi, A. A., and Chamorovsky, Y. K., "Optical fibres and fibre tapers with an array of bragg gratings," Quantum Electronics **49**, 1127-1131 (2019).
[7] Boivinet, S., Lecourt, J. B., Hernandez, Y., Fotiadi, A. A., Wuilpart, M., and Megret, P., "All-fiber 1-μm pm mode-lock laser delivering picosecond pulses at sub-mhz repetition rate," IEEE Photonics Technology Letters **26**, 2256-2259 (2014).
[8] Kuznetsov, M. S., Antipov, O. L., Fotiadi, A. A., and Mégret, P., "Electronic and thermal refractive index changes in ytterbium-doped fiber amplifiers," Opt. Express **21**, 22374 (2013).
[9] Phan Huy, K., Nguyen, A. T., Brainis, E., Haelterman, M., Emplit, P., Corbari, C., Canagasabey, A., Kazansky, P. G., Deparis, O., Fotiadi, A. A., Mégret, P., and Massar, S., "Photon pair source based on parametric fluorescence in periodically poled twin-hole silica fiber," Opt. Express **15**, 4419 (2007).
[10] Udd, E., Du, H. H., and Wang, A., "Fiber optic sensors and applications vi," in *Fiber Optic Sensors and Applications VI*(2009).
[11] Barrias, A., Casas, J. R., and Villalba, S., "A review of distributed optical fiber sensors for civil engineering applications," Sensors **16**, 748 (2016).
[12] Galindez-Jamioy, C. A., and López-Higuera, J. M., "Brillouin distributed fiber sensors: An overview and applications," Journal of Sensors **2012**, 1-17 (2012).
[13] Soto, M. A., [Distributed brillouin sensing: Time-domain techniques], Springer, Singapore (2018).
[14] Marpaung, D., Pagani, M., Morrison, B., and Eggleton, B. J., "Nonlinear integrated microwave photonics," Journal of Lightwave Technology **32**, 3421-3427 (2014).
[15] Eggleton, B. J., Poulton, C. G., Rakich, P. T., Steel, M. J., and Bahl, G., "Brillouin integrated photonics," Nature Photonics, 1-14 (2019).
[16] Li, J., Suh, M.-G., and Vahala, K., "Microresonator brillouin gyroscope," Optica **4**, 346-348 (2017).
[17] Faustov, A. V., Gusarov, A. V., Mégret, P., Wuilpart, M., Zhukov, A. V., Novikov, S. G., Svetukhin, V. V., and Fotiadi, A. A., "The use of optical frequency-domain reflectometry in remote distributed measurements of the γ-radiation dose," Technical Physics Letters **41**, 414-417 (2015).
[18] Faustov, A. V., Gusarov, A. V., Mégret, P., Wuilpart, M., Zhukov, A. V., Novikov, S. G., Svetukhin, V. V., and Fotiadi, A. A., "Application of phosphate doped fibers for ofdr dosimetry," Results in Physics **6**, 86-87 (2016).
[19] Faustov, A. V., Gusarov, A., Wuilpart, M., Fotiadi, A. A., Liokumovich, L. B., Zolotovskiy, I. O., Tomashuk, A. L., de Schoutheete, T., and Megret, P., "Comparison of gamma-radiation induced attenuation in al-doped, p-doped and ge-doped fibres for dosimetry," IEEE Transactions on Nuclear Science **60**, 2511-2517 (2013).
[20] Faustov, A. V., Gusarov, A., Liokumovich, L. B., Fotiadi, A. A., Wuilpart, M., and Mégret, P., "Comparison of simulated and experimental results for distributed radiation-induced absorption measurement using ofdr reflectometry," (2013), p. 87943O.

[21] Morana, A., Planes, I., Girard, S., Cangialosi, C., Delepine-Lesoille, S., Marin, E., Boukenter, A., and Ouerdane, Y., "Steady-state radiation-induced effects on the performances of botda and botdr optical fiber sensors," IEEE Transactions on Nuclear Science **65**, 111-118 (2017).
[22] Dong, Y., Jiang, T., Teng, L., Zhang, H., Chen, L., Bao, X., and Lu, Z., "Sub-mhz ultrahigh-resolution optical spectrometry based on brillouin dynamic gratings," Optics letters **39**, 2967-2970 (2014).
[23] Fotiadi, A. A., Brambilla, G., Ernst, T., Slattery, S. A., and Nikogosyan, D. N., "Tpa-induced long-period gratings in a photonic crystal fiber: Inscription and temperature sensing properties," Journal of the Optical Society of America B: Optical Physics **24**, 1475-1481 (2007).
[24] Caucheteur, C., Fotiadi, A., Megret, P., Slattery, S. A., and Nikogosyan, D. N., "Polarization properties of long-period gratings prepared by high-intensity femtosecond 352-nm pulses," IEEE Photonics Technology Letters **17**, 2346-2348 (2005).
[25] Petermann, K., [Laser diode modulation and noise], Springer Science & Business Media (2012).
[26] Ohtsubo, J., [Semiconductor lasers: Stability, instability and chaos], Springer (2012).
[27] Galiev, R., Pavlov, N., Kondratiev, N., Koptyaev, S., Lobanov, V., Voloshin, A., Gorodnitskiy, A., and Gorodetsky, M., "Spectrum collapse, narrow linewidth, and bogatov effect in diode lasers locked to high-q optical microresonators," Opt. Express **26**, 30509-30522 (2018).
[28] Liang, W., Ilchenko, V., Eliyahu, D., Savchenkov, A., Matsko, A., Seidel, D., and Maleki, L., "Ultralow noise miniature external cavity semiconductor laser," Nature communications **6**, 1-6 (2015).
[29] Wei, F., Yang, F., Zhang, X., Xu, D., Ding, M., Zhang, L., Chen, D., Cai, H., Fang, Z., and Xijia, G., "Subkilohertz linewidth reduction of a dfb diode laser using self-injection locking with a fiber bragg grating fabry-perot cavity," Opt. Express **24**, 17406-17415 (2016).
[30] Korobko, D. A., Zolotovskii, I. O., Panajotov, K., Spirin, V. V., and Fotiadi, A. A., "Self-injection-locking linewidth narrowing in a semiconductor laser coupled to an external fiber-optic ring resonator," Optics Communications **405**, 253-258 (2017).
[31] Spirin, V., López-Mercado, C., Mégret, P., and Fotiadi, A., "Single-mode brillouin fiber laser passively stabilized at resonance frequency with self-injection locked pump laser," Laser Physics Letters **9**, 377 (2012).
[32] Bueno Escobedo, J. L., Spirin, V. V., López-Mercado, C. A., Mégret, P., Zolotovskii, I. O., and Fotiadi, A. A., "Self-injection locking of the dfb laser through an external ring fiber cavity: Polarization behavior," Results in Physics **6**, 59-60 (2016).
[33] López-Mercado, C. A., Spirin, V. V., Bueno Escobedo, J. L., Márquez Lucero, A., Mégret, P., Zolotovskii, I. O., and Fotiadi, A. A., "Locking of the dfb laser through fiber optic resonator on different coupling regimes," Optics Communications **359**, 195-199 (2016).
[34] Bao, X., and Chen, L., "Recent progress in brillouin scattering based fiber sensors," Sensors **11**, 4152-4187 (2011).
[35] Y. Dong, H. Z., Z. Lu, L. Chen, and X. Bao, "Long-range and high-spatial-resolution distributed birefringence measurement of a polarization-maintaining fiber based on brillouin dynamic grating," Journal of Lightwave Technology **31**, 2681-2686 (2013).
[36] Angulo-Vinuesa, X., Dominguez-Lopez, A., Lopez-Gil, A., Ania-Castañón, J. D., Martin-Lopez, S., and Gonzalez-Herraez, M., "Limits of botda range extension techniques," IEEE Sensors Journal **16**, 3387-3395 (2016).
[37] Spirin, V. V., Kellerman, J., Swart, P. L., and Fotiadi, A. A., "Intensity noise in sbs with injection locking generation of stokes seed signal," Opt. Express **14**, 8328 (2006).
[38] Denisov, A., Soto, M. A., and Thévenaz, L., "Going beyond 1000000 resolved points in a brillouin distributed fiber sensor: Theoretical analysis and experimental demonstration," Light: Science & Applications **5**, e16074-e16074 (2016).
[39] Spirin, V. V., Castro, M., López-Mercado, C. A., Mégret, P., and Fotiadi, A. A., "Optical locking of two semiconductor lasers through high-order brillouin stokes components in optical fiber," Laser Physics **22**, 760-764 (2012).
[40] Antman, Y., Primerov, N., Sancho, J., Thevenaz, L., and Zadok, A., "Localized and stationary dynamic gratings via stimulated brillouin scattering with phase modulated pumps," Opt. Express **20**, 7807-7821 (2012).
[41] Peled, Y., Motil, A., Kressel, I., and Tur, M., "Monitoring the propagation of mechanical waves using an optical fiber distributed and dynamic strain sensor based on botda," Opt. Express **21**, 10697-10705 (2013).
[42] Zadok, A., Antman, Y., Primerov, N., Denisov, A., Sancho, J., and Thevenaz, L., "Random-access distributed fiber sensing," Laser & Photonics Reviews **6**, L1-L5 (2012).
[43] Motil, A., Bergman, A., and Tur, M., "[invited] state of the art of brillouin fiber-optic distributed sensing," Optics & Laser Technology **78**, 81-103 (2016).

[44] Sovran, I., Motil, A., and Tur, M., "Frequency-scanning botda with ultimately fast acquisition speed," IEEE Photonics Technology Letters **27**, 1426-1429 (2015).
[45] Preda, C. E., Fotiadi, A. A., and Megret, P., "Numerical approximation for brillouin fiber ring resonator," Opt Express **20**, 5783-5788 (2012).
[46] Zhang, H., Zhou, D., Wang, B., Pang, C., Xu, P., Jiang, T., Ba, D., Li, H., and Dong, Y., "Recent progress in fast distributed brillouin optical fiber sensing," Applied Sciences **8** (2018).
[47] Lopez-Mercado, C. A., Korobko, D. A., Zolotovskii, I. O., and Fotiadi, A. A., "Application of dual-frequency self-injection locked dfb laser for brillouin optical time domain analysis," Sensors **21**, 6859 (2021).
[48] Spirin, V. V., Mégret, P., and Fotiadi, A. A., "Passively stabilized doubly resonant brillouin fiber lasers," Fiber Laser, 89 (2016).
[49] Otterstrom, N. T., Behunin, R. O., Kittlaus, E. A., Wang, Z., and Rakich, P. T., "A silicon brillouin laser," Science **360**, 1113-1116 (2018).
[50] Peled, Y., Motil, A., and Tur, M., "Fast brillouin optical time domain analysis for dynamic sensing," Opt. Express **20**, 8584-8591 (2012).
[51] López-Mercado, C. A., Spirin, V. V., Kablukov, S. I., Zlobina, E. A., Zolotovskiy, I. O., Mégret, P., and Fotiadi, A. A., "Accuracy of single-cut adjustment technique for double resonant brillouin fiber lasers," Optical Fiber Technology **20**, 194-198 (2014).
[52] Spirin, V. V., Bueno Escobedo, J. L., Miridonov, S. V., Maya Sánchez, M. C., López-Mercado, C. A., Korobko, D. A., Zolotovskii, I. O., and Fotiadi, A. A., "Sub-kilohertz brillouin fiber laser with stabilized self-injection locked dfb pump laser," Optics & Laser Technology **141**, 107156 (2021).
[53] Korobko, D., Zolotovskii, I., Svetukhin, V., Zhukov, A., Fomin, A., Borisova, C., and Fotiadi, A., "Detuning effects in brillouin ring microresonator laser," Opt. Express **28**, 4962-4972 (2020).
[54] Spirin, V. V., Bueno Escobedo, J. L., Korobko, D. A., Mégret, P., and Fotiadi, A. A., "Stabilizing dfb laser injection-locked to an external fiber-optic ring resonator," Opt. Express **28**, 478-484 (2020).
[55] Hansch, T., and Couillaud, B., "Laser frequency stabilization by polarization spectroscopy of a reflecting reference cavity," Optics communications **35**, 441-444 (1980).
[56] Alnis, J., Matveev, A., Kolachevsky, N., Udem, T., and Hänsch, T., "Subhertz linewidth diode lasers by stabilization to vibrationally and thermally compensated ultralow-expansion glass fabry-pérot cavities," Physical Review A **77**, 053809 (2008).
[57] Derickson, D., Hentschel, C., and Vobis, J., [Fiber optic test and measurement], Prentice Hall PTR New Jersey (1998).
[58] Richter, L. E., Mandelberg, H. I., Kruger, M. S., and Mcgrath, P. A., "Linewidth determination from self-heterodyne measurements with subcoherence delay times," Ieee Journal of Quantum Electronics **22**, 2070-2074 (1986).
[59] Mercer, L. B., "1 /f frequency noise effects on self-heterodyne linewidth measurements," IEEE Lightwave Technology **9**, 485-493 (1991).
[60] Horak, P., and Loh, W. H., "On the delayed self-heterodyne interferometric technique for determining the linewidth of fiber lasers," Opt Express **14**, 3923-3928 (2006).
[61] Chen, M., Meng, Z., Wang, J., and Chen, W., "Ultra-narrow linewidth measurement based on voigt profile fitting," Opt. Express **23**, 6803-6808 (2015).
[62] Di Domenico, G., Schilt, S., and Thomann, P., "Simple approach to the relation between laser frequency noise and laser line shape," Applied Optics **49**, 4801-4807 (2010).
[63] Li, Y., Fu, Z., Zhu, L., Fang, J., Zhu, H., Zhong, J., Xu, P., Chen, X., Wang, J., and Zhan, M., "Laser frequency noise measurement using an envelope-ratio method based on a delayed self-heterodyne interferometer," Optics Communications **435**, 244-250 (2019).
[64] Bueno Escobedo, J. L., Spirin, V. V., López-Mercado, C. A., Márquez Lucero, A., Mégret, P., Zolotovskii, I. O., and Fotiadi, A. A., "Self-injection locking of the dfb laser through an external ring fiber cavity: Application for phase sensitive otdr acoustic sensor," Results in Physics **7**, 641-643 (2017).
[65] Gorshkov, B. G., Yüksel, K., Fotiadi, A. A., Wuilpart, M., Korobko, D. A., Zhirnov, A. A., Stepanov, K. V., Turov, A. T., Konstantinov, Y. A., and Lobach, I. A., "Scientific applications of distributed acoustic sensing: State-of-the-art review and perspective," Sensors **22**, 1033 (2022).
[66] Lu, Y., Zhu, T., Chen, L., and Bao, X., "Distributed vibration sensor based on coherent detection of phase-otdr," Journal of Lightwave Technology **28**, 3243-3249 (2010).
[67] Muanenda, Y., Oton, C. J., Faralli, S., and Di Pasquale, F., "A cost-effective distributed acoustic sensor using a commercial off-the-shelf dfb laser and direct detection phase-otdr," IEEE Photonics Journal **8**, 1-10 (2016).

[68] Zhong, X., Zhao, S., Deng, H., Gui, D., Zhang, J., and Ma, M., "Nuisance alarm rate reduction using pulse-width multiplexingφ-otdr with optimized positioning accuracy," Optics Communications **456**, 124571 (2020).
[69] Kbashi, H. J., Sergeyev, S. V., Al-Araimi, M., Rozhin, A., Korobko, D., and Fotiadi, A., "High-frequency vector harmonic mode locking driven by acoustic resonances," Optics Letters **44**, 5112-5115 (2019).
[70] Bueno Escobedo, J. L., Jason, J., López-Mercado, C. A., Spirin, V. V., Wuilpart, M., Mégret, P., Korobko, D. A., Zolotovskiy, I. O., and Fotiadi, A. A., "Distributed measurements of vibration frequency using phase-otdr with a dfb laser self-stabilized through pm fiber ring cavity," Results in Physics **12**, 1840-1842 (2019).
[71] Xu, S., Qin, Z., Zhang, W., and Xiong, X., "Monitoring vehicles on highway by dual-channel φ-otdr," Applied Sciences **10**, 1839 (2020).